Journal of The Electrochemical Society, **150** (7) G412-G417 (2003)
0013-4651/2003/150(7)/G412/6/$7.00 © The Electrochemical Society, Inc.

Plastic-Compatible Low Resistance Printable Gold Nanoparticle Conductors for Flexible Electronics

Daniel Huang,[a] Frank Liao,[b] Steven Molesa,[b] David Redinger,[b] and Vivek Subramanian[b,z]

[a]*Department of Bioengineering,* [b]*Department of Electrical Engineering and Computer Sciences, University of California, Berkeley, California 94720, USA*

Low resistance conductors are crucial for the development of ultra-low-cost electronic systems such as radio frequency identification tags. Low resistance conductors are required to enable the fabrication of high-*Q* inductors, capacitors, tuned circuits, and interconnects. The fabrication of these circuits by printing will enable a dramatic reduction in cost, through the elimination of lithography, vacuum processing, and the need for high-cost substrates. Solutions of organic-encapsulated gold nanoparticles many be printed and subsequently annealed to form low resistance conductor patterns. We describe a process to form the same, and discuss the optimization of the process to demonstrate plastic-compatible gold conductors for the first time. By optimizing both the size of the nanoparticle and the length of the alkanethiol encapsulant, it is possible to produce particles that anneal at low temperatures (<150°C) to form continuous gold films having low resistivity. We demonstrate the printing of these materials using an inkjet printer to demonstrate a plastic-compatible low resistance conductor technology.
 [DOI: 10.1149/1.1582466]

Manuscript submitted September 23, 2002; revised manuscript received February 3, 2003. Available electronically May 30, 2003.

In recent years, there has been tremendous interest in flexible electronics. Besides the obvious applications of flexible electronics in flat panel displays,[1] flexible circuits are also promising for use in such applications as radio frequency identification (RFID) tags,[2] low cost sensors,[3] and other disposable electronic devices. In particular, devices based on organic semiconductors are considered to be very promising for these applications since they may potentially be fabricated entirely using printing technologies,[4] eliminating the need for such major cost points as lithography, vacuum processing including physical vapor deposition, plasma etching, and chemical vapor deposition (CVD), while simultaneously allowing the use of reel-to-reel processing, resulting in reduced substrate handling and cleanroom costs as well. Furthermore, since printing is inherently additive in nature, material and disposal costs are also expected to be reduced, resulting in an extremely low net system cost.

Progress in organic semiconductor technology has been rapid, with carrier mobilities improving in a sustained fashion over the last decade.[5-7] Indeed, the performance of various solution processed organic semiconductor materials has reached a state where circuit demonstrations are now possible. While several demonstration circuits have been fabricated using organic semiconductors, including shift registers, multiplexers, display backplanes, and encoders,[2,8] little work has been done on the other piece of the circuit puzzle, namely, the passive components. The requirements for these components are tremendous, both in terms of performance and cost. RFID applications will require the printing of high-*Q* inductors, transformers, and tuned circuits.[9] Display applications including both active matrix liquid crystal displays (AMLCDs) and organic light emitting diode (OLED) displays will require the printing of low resistance interconnects. Furthermore, organic transistors require work function-matched contacts. Evaporated gold is commonly used for these circuits, but is too expensive for use in low cost reel-to-reel applications. What is required, therefore, is a low resistance conductor technology suitable for printing using such technologies as screen printing and inkjet printing. This technology must be compatible with organic electronic devices, in that it must be possible to fabricate these low resistance structures at low temperatures. Specifically, many common low cost plastics deform unacceptably between 150 and 200°C. Therefore, any printed conductor technology must have a maximum temperature excursion lower than this range.

It has been known for some time that metal nanoclusters have reduced melting and sintering temperatures when compared to their bulk counterparts.[10] Monolayer protected clusters (MPCs) of gold protected by alkanethiols can be dissolved into common nonpolar solvents such as toluene, THF, and hexanes, and are therefore suitable for printing. Their low sintering temperatures make them potentially suitable for use in electronics in plastic, since they may potentially be annealed at low temperatures to form low resistance conductor films. Thiol-derivatized gold nanoclusters have been used in numerous interdisciplinary applications ranging from biological marking to nanotechnology.[11,12] Unfortunately, the melting/sintering temperatures for all gold nanocrystals reported to date are greater than 200°C, making them unsuitable for use in electronics on plastic applications. In this paper, we demonstrate a thiol-derivatized gold nanocluster technology suitable for use in printed circuits on plastic. We demonstrate, for the first time, a plastic-compatible gold nanocrystal technology with a temperature excursion of less than 150°C. Using a systematic study of the nanoparticle synthesis parameters, we demonstrate the optimization of the same to achieve low anneal temperatures while maintaining low film resistance.

Experimental

To enable the optimization of the conductor process, gold nanocrystals were synthesized with varying diameter and encapsulant species. After synthesis and purification, the nanocrystals were dissolved in a solvent and dispensed onto plastic substrates by micropipetting or inkjet printing. Upon drying, the resulting films (which are nonconductive as deposited due to the presence of the insulating alkanethiols) were annealed to form a low resistance conductor patterns. The various transition temperatures associated with the anneal process and the final resistance were measured and related to the synthesis and anneal conditions to establish optimization guidelines, enabling the development of a low temperature conductor process. The entire process is described in detail below.

Nanocrystal synthesis.—The synthesis of the gold nanoclusters followed that reported by Murray.[13] Here, we studied the effect of nanocrystal size. We varied the length of the alkanethiol molecules that was used as the encapsulant, and also adjusted the size of the resulting nanocrystal by controlling the relative mole ratio of the encapsulant and gold.

In brief, 1.5 g of tetroactylammonium bromide was mixed with 80 mL of toluene and added to 0.31 g of $HAuCl_4:xH_2O$ in 25 mL of deionized (DI) water. $AuCl4^-$ was transferred into the toluene and the aqueous phase was removed. A calculated mole ratio of an alkanethiol was added to the gold solution. Thiols with lengths rang-

[z] E-mail: viveks@eecs.berkeley.edu

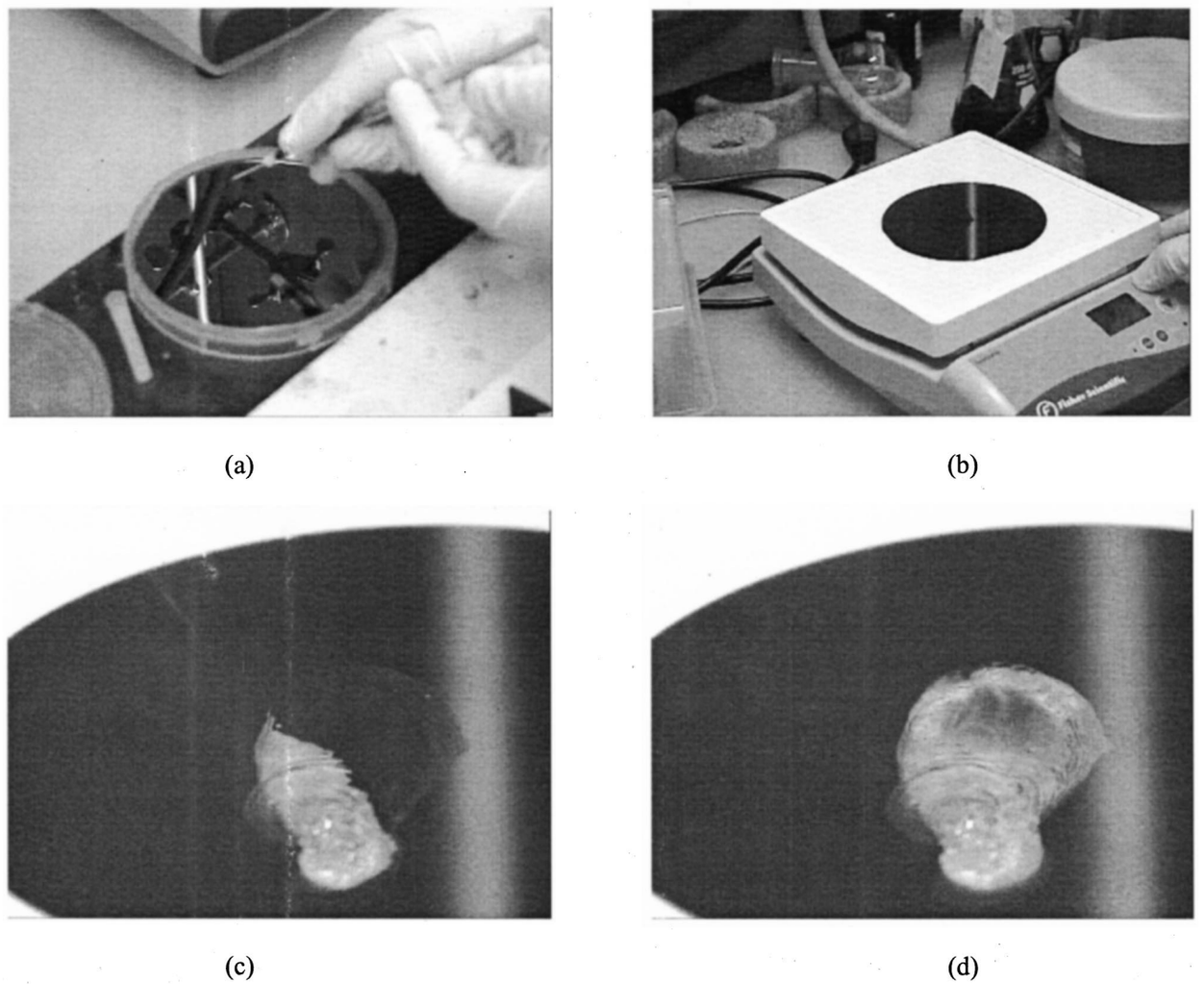

Figure 1. Sequence of chemical modifications during gold deposition and anneal: (a) the gold is deposited as a solution. (b) After the solvent evaporates, the resulting black nonconductive film is heated. (c) The alkanethiol encapsulant sublimates and (d) the gold nanoparticles coalesce to for a continuous gold film.

ing from 4 carbon atoms to 12 carbon atoms were used. For crystals with larger diameters (~5 nm average diam), a thiol:gold mole ratio of 1/12:1 was used. For smaller diameters, nanocrystals (~1.5 nm av diam), a thiol:gold mole ratio of 4:1 was used. Sodium borohydride mixed in 25 mL of water was added into the organic phase with a fast addition over approximately 10 s. The mixture reacted at room temperature for three and a half hours. The toluene was removed with a rotary evaporator and the leftover black particles suspended in ethanol and sonicated briefly. The particles were washed with ethanol and acetone and air dried.

Heating tests.—The gold nanocrystals were redissolved in toluene to form saturated solutions. To measure resistance, the solutions were then micropipetted onto an insulating substrate (either plastic or SiO_2) and allowed to air dry. To confirm plastic compatibility, several commercial plastics were used. Commercial polyester films (the smooth side of 3M inkjet transparencies and the uncoated side of laser printer transparencies) generally had deformation temperatures in the range of 150-180°C, where we defined the deformation temperature as the temperature at which the film underwent dramatic contraction. Typically, these films showed significant degradation in transparency at temperatures 10-20°C lower, which therefore represented an upper bound on the usable temperature range for these materials, depending on their application. Therefore, these films were used only for the lower temperature tests. For these tests, the micropipetted film was dispensed on the uncoated surface of the polyester films, distributed by 3M as inkjet transparency film. For heating tests involving higher temperatures, Dupont Melinex films based on a polyethylene terephthalate base were used. These films were found to survive temperature excursions as high as 200°C and higher without undergoing substantial surface deformation. On these high temperature plastics, the full range of experiments were performed. Importantly, no substantial difference in resistivity or conversion temperature was noted between the various plastics for these micropipetted patterns. After the micropipetted solution had dried, the resulting nonconductive black film was then heated on a hotplate equipped with a surface probe to ensure accurate temperature measurement. Upon application of adequate heat, the film converted to a continuous gold conductor. This happened through a two-step process, involving the sublimation of the alkanethiol, followed by the melting, coagulation, and immediate solidification of the gold nanoparticles to form continuous gold films. The anneal process is shown in Fig. 1.

A ramped anneal was performed to determine the various transition temperatures. The thiol burnoff temperature was determined visually, by a rapid transition of the film color from black to gold, accompanied by a sublimation of the thiol in the form of a black

Table I. Multifactorial screening design used to determine effect of anneal and deposition parameters on transition temperatures and film resistivity.

Pattern	Deposition temperature (°C)	Postanneal[b] temperature (°C)	Particle size (nm)	Alkanethiol carbon chain length	Anneal ambient
−−−−+	RT[a]	Melt	1.5	4	Air
−−−+−	RT	Melt	1.5	6	N2
−−+−−	RT	Melt	5	4	N2
−−+++	RT	Melt	5	6	Air
−+−−−	RT	Melt + 20	1.5	4	N2
−+−++	RT	Melt + 20	1.5	6	Air
−++−+	RT	Melt + 20	5	4	Air
−+++−	RT	Melt + 20	5	6	N2
+−−−−	150	Melt	1.5	4	N2
+−−++	150	Melt	1.5	6	Air
+−+−+	150	Melt	5	4	Air
+−++−	150	Melt	5	6	N2
++−−+	150	Melt + 20	1.5	4	Air
++−+−	150	Melt + 20	1.5	6	N2
+++−−	150	Melt + 20	5	4	N2
+++++	150	Melt + 20	5	6	Air

[a] RT is Room temperature (~300 K).
[b] Postanneals were performed to reduce resistivity. Postanneal condition was predetermined from the melt temperature measured during the ramped temperature transition measurements.

smoke. Upon further annealing, the film underwent a color transition from a dull golden color to a shiny gold. This indicated the nanocrystal melting temperature. At this point, the film achieves a low resistance state. Resistivity of the films were measured using a four-point probe and an HP4156 semiconductor parameter analyzer.

To study the effect of various experimental conditions, a multifactorial design of experiments was used to screen for the effects of various parameters on the transition temperatures and final film resistivity. The studied parameters were nanocrystal size, encapsulation carbon chain length, anneal ambient, and postanneal conditions. The experimental design is shown in Table I. Using the results of the screening design, an optimized nanocrystal synthesis and anneal process was selected. Using this process, low resistance inkjetted conductor lines were printed. For a 1 μm thick line, a sheet resistance of less than 0.03Ω/□ was achieved, indicating a conductivity of approximately 70% of bulk gold, attesting to the robustness of this process. An atomic force micrograph of the inkjetted line is shown in Fig. 2. The entire process was performed at low temperature (maximum temperature excursion of 140°C using the hexanethiol-encapsulated nanoparticles) on the uncoated surface of the low temperature commercial polyester-based plastic described above. It is important to note that the toluene solvent does in fact attack the plastics used herein; however, the actual volumes of solution used during injetting are extremely small (typical drop sizes were <40 pL), facilitating rapid evaporation of the toluene. Therefore, no damage to the plastic substrate was found to occur. The enhanced evaporation of the toluene was facilitated by maintaining the substrate at an elevated temperature during jetting. In general, the adhesion of the inkjetted lines to the polyester was found to be

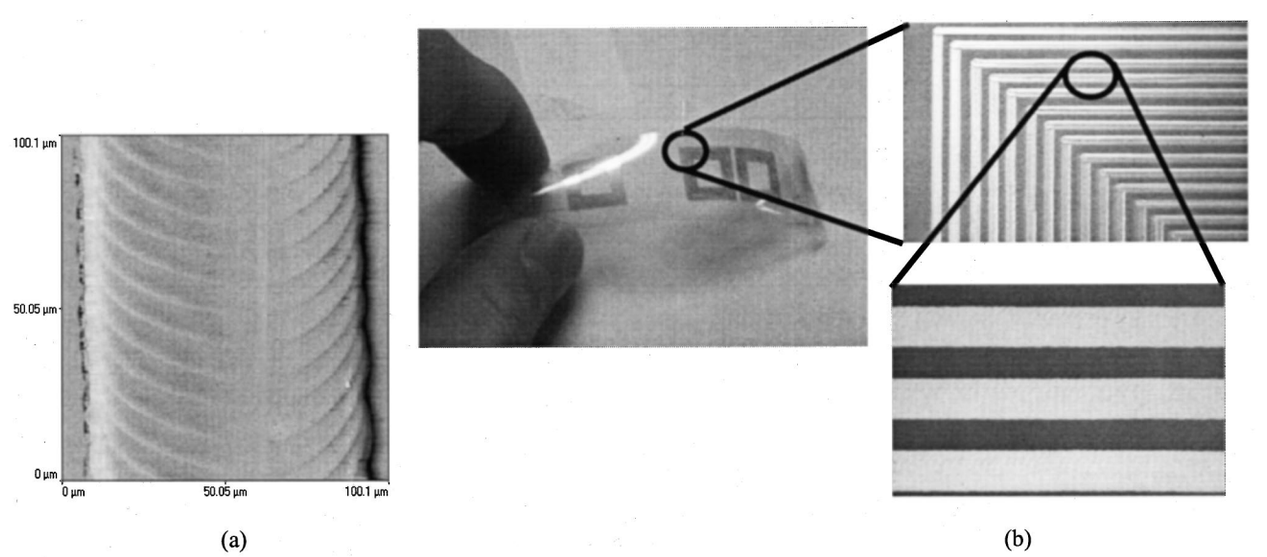

Figure 2. (a) Atomic force micrograph of an inkjetted line. (b) Optical micrographs of an inkjetted inductor formed on commercial polyester-based general purpose transparency plastic.

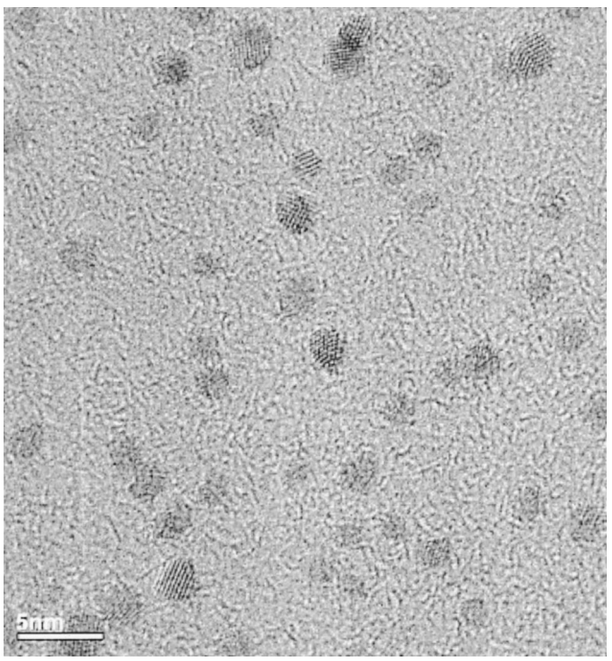

Figure 3. Transmission electron micrographs of hexanethiol-encapsulated nanocrystals synthesized with a gold: thiol mole ratio of 1:4, resulting in an average particle diam of ~2 nm.

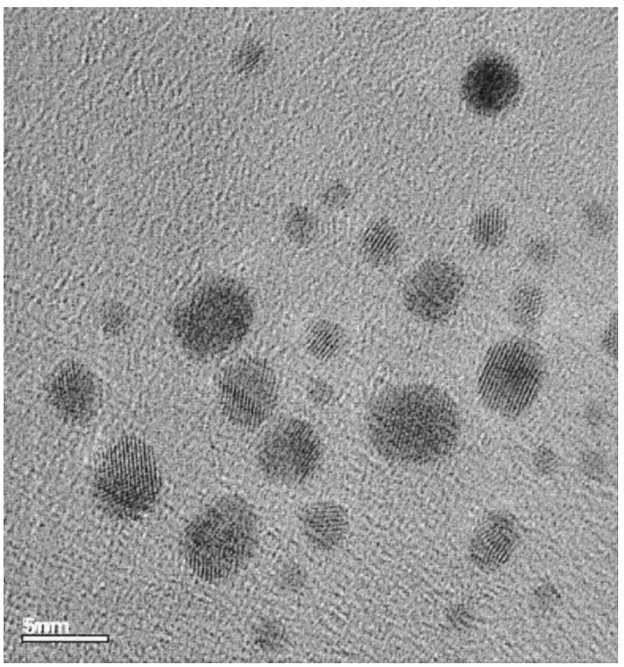

Figure 4. Transmission electron micrographs of hexanethiol-encapsulated nanocrystals synthesized with a gold: thiol mole ratio of 1:1/12, resulting in an average particle diam of ~5 nm.

fairly good. The adhesion was found to be a strong function of the temperature of the substrate during jetting. In general, it was found that adhesion improved dramatically when the temperature of the substrate was raised close to the thiol sublimation temperature. The reason for this improved adhesion is currently under investigation. It is suspected that some thiol remains as an interfacial layer between the plastic and the gold, improving the adhesion.

Results and Discussion

To determine the size of the nanocrystals, dilute solutions of the same were deposited on copper grids and analyzed using transmission electron microscopy. Figures 3 and 4 show transmission electron micrographs of hexanethiol-encapsulated nanocrystals synthesized with gold: thiol concentrations of 1:4 and 1:1/12, respectively. As reported by Murray *et al.*,[13] there is a distribution of sizes for the different concentrations of thiols used. The 1:4 ratio gives smaller nanoclusters of a size of approximately 1.5 nm in diam and a relatively tight distribution in diameter. The 1:1/12 ratio of gold to thiol gives a wider distribution, with an average diam of 5 nm.

Table II shows the results of the annealing tests. From this table, it is apparent that the required anneal temperature is a strong function of the encapsulant carbon chain length. Nanocrystals encapsulated in dodecanethiol anneal at 170-200°C, which is not plastic compatible. However, by reducing the carbon chain length to four or six, it is possible to obtain nanocrystals that anneal at temperatures compatible with many low cost plastics. Interestingly, it is also apparent that the larger nanocrystals have lower anneal temperature requirements. This is unexpected, since it is known that the melt temperature of individual 1.5 nm diam nanocrystals is lower than that of the 5 nm diam nanocrystals. We explain this behavior based on the fact that the volume fraction of encapsulant is significantly larger in the 1.5 diam particles, and therefore, using the same ramped anneal process, a higher temperature is required to completely burn off the encapsulant. The effect of encapsulation carbon chain length on the various transition temperatures is shown in Fig. 5 and 6, which show the variation in the various transition temperatures as a function of carbon chain length for 1.5 and 5 nm nanocrystals, respectively. It is important to note that nanocrystals formed with both butanethiol and hexanethiol have transition temperatures in the commercially important plastic-compatible range. To our knowledge, this is the first time that such a low anneal temperature nanocrystal process has been reported.

To screen for the effects of the various synthesis and anneal parameters on the anneal temperature requirements, a multifactorial screening design was used. The design (shown in Table I), was established to identify first-order effects and most two-parameter interactions. The temperature at which conduction occurred was used as a response. The response of this parameter to alkanethiol carbon chain length, particle diameter, deposition temperature, and anneal ambient is shown in Fig. 7 (the linearity of the plots is due to the identification of first-order effects and interactions only). Only carbon chain length and particle diameter had a significant impact on the temperature at which conduction occurred. All other parameters (deposition temperature, anneal ambient, and postanneal temperature) did not have significant impact upon the temperature at which conduction occurred. This is expected, since the encapsulant was removed through a sublimation process, and was therefore essentially independent of these factors. As in the previous experi-

Table II. Variation in transition temperatures during anneal as a function of encapsulant chain length and nanoparticle size.

	5 nm particles (1:1/12th mole ratio)		
Encapsulant	Thiol sublimation temperature (°C)	Au coalescence temperature (°C)	Conduction temperature (°C)
Dodecanethiol	170-180	170-180	170-180
Octanethiol	160-172	160-172	170
Hexanethiol	100	120	150
Butanethiol	120	120	120
	1.5 nm particles (1:4 mole ratio)		
Dodecanethiol	190	190	190
Octanethiol	168-180	168-180	175
Hexanethiol	169	175	175
Butanethiol	127	127-137	133

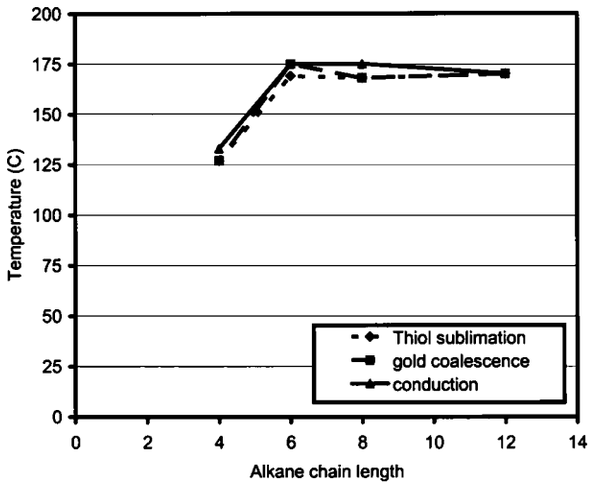

Figure 5. Variation in the various transition temperatures as a function of carbon chain length for 1.5 nm nanocrystals.

ment, the temperature at which conduction occurred showed a strong dependence on carbon chain length, and some dependence on nanocrystal size. As above, the larger nanocrystals appeared to have a reduced temperature at which conduction occurs; this is again explained by the substantially larger volume fraction of encapsulant that must be sublimated for the smaller nanoparticles.

The variation in final resistivity as a function of the various synthesis and anneal perimeters was studied also. The final resistivity appeared to be essentially independent of synthesis conditions, provided a sufficient anneal was used to completely drive off the majority of the encapsulant species. The presence of a sufficient anneal appears to be the crucial parameter in achieving low resistance films. A 30 min anneal at the melting temperature was found to substantially reduce the resistance. A similar effect was also achieved by using an anneal at 20°C above the melting temperature for a shorter time (on the order of 2-3 min). Tests performed on various low cost plastics indicate that both butanethiol and hexanethiol encapsulated species may be used to form low resistance conductors on these substrates. The choice of encapsulant can be

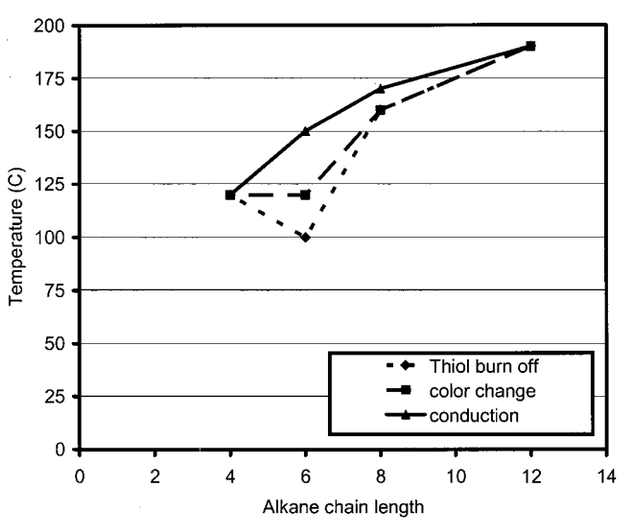

Figure 6. Variation in the various transition temperatures as a function of carbon chain length for 5 nm nanocrystals.

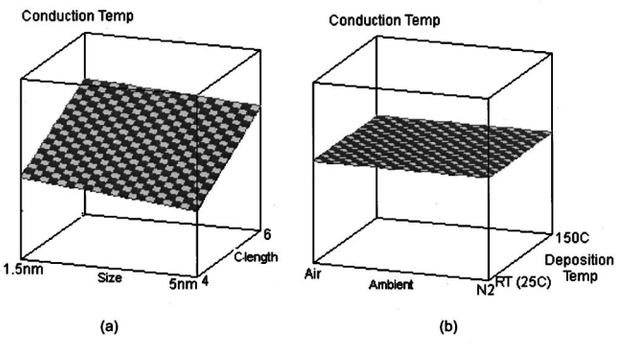

Figure 7. Response characterization of conduction temperature to (a) alkanethiol carbon chain length and (b) deposition temperature and anneal ambient.

made based on the maximum temperature excursion allowed for the plastic in question.

It is important to note that the anneal temperatures determined above were measured for fairly thick films, several micrometers thick. For thinner films, on the order of 1 μm, anneal temperatures were depressed across the board by approximately 20°C. This again attests to the fact that the removal of the encapsulant is the limiting factor in forming low resistance conductors. The inkjetted line shown in Fig. 2 has a sheet resistance of 0.03 Ω/□ for a 1 μm thick film. The entire process is performed at a maximum temperature of approximately 150°C.

Some tests on stability were also performed. In general, the shelf life of the short carbon chain nanocrystals was reduced, unless the nanocrystals were stored in a refrigerated state. This reduced shelf life was caused by the continuous evaporation of the encapsulant, resulting in nanocrystal degradation through reduction in solubility. Furthermore, the larger nanocrystals were also found to have shorter lifetimes, again due to encapsulant evaporation. Since the larger nanocrystals had a smaller volume fraction of encapsulant, they were more sensitive to environmental degradation. The most promising candidate for printed conductors appears to be the 1.5 nm particles encapsulated with hexanethiol. Inkjet printed films have anneal temperatures less than 150°C, which are plastic compatible. The nanocrystals also have excellent stability, lasting several months in powder form without degradation.

Conclusions

In this paper, for the first time, we have demonstrated a plastic-compatible printed conductor process using gold nanocrystals. By reducing the alkane chain length we can significantly lower the processing temperature requirements necessary to convert solution-deposited nanoparticles into low resistance, continuous films. Using 4- or 6-carbon chain length thiols, it is possible to produce nanocrystals that anneal at plastic-compatible temperatures. The anneal conditions are independent of anneal ambient, and low resistance films are uniformly achieved provided a sufficient anneal is used to completely drive off the encapsulant. There is a tradeoff between stability and anneal temperature due to the instability of thiols with short alkane chains. However, optimization of the process reveals that 1.5 nm gold nanoclusters encapsulated with hexanethiol have good stability and are suitable for use as printed conductors on plastic. Inkjet-printed conductor patterns formed on plastic using this material result in low resistance lines with conductivities as high as 70% of bulk gold, attesting to the quality of this process.

Acknowledgments

This research was jointly sponsored in part under SRC contract 01-MC-460 and DARPA grant MD972-01-1-0021.

The University of California at Berkeley assisted in meeting the publication costs of this article.

References

1. H. Klauk, B. D'Andrade, and T. N. Jackson, in the *57th Annual Device Research Conference Digest*, IEEE, p. 162, (1999).
2. B. K. Crone, A. Dodabalapur, R. Sarpeshkar, R. W. Filas, Y.-Y. Lin, and Z. Bao, *Appl. Phys. Lett.*, **89**, 5125 (2001).
3. B. Crone, A. Dodabalapur, A. Gelperin, L. Torsi, H. E. Katz, and A. J. Lovinger, *Appl. Phys. Lett.*, **78**, 2229 (2001).
4. V. Subramanian, Paper presented at the Half Moon Bay Maskless Lithography Workshop, DARPA/SRC, Half Moon Bay, CA, Nov 9-10, 2000.
5. A. Tsumura, H. Koezuka, and T. Ando, *Appl. Phys. Lett.*, **49**, 1210 (1986).
6. A. Assadi, C. Svensson, M. Willander, and O. Inganäs, *Appl. Phys. Lett.*, **53**, 195 (1988).
7. H. Sirringhaus, N. Tessler, and R. H. Friend, *Science (Washington, DC, U.S.)*, **280**, 1741 (1998).
8. G. H. Gelinck, T. C. T. Genus, and D. M. de Leeuw, *Appl. Phys. Lett.*, **77**, 1487 (2000).
9. K. Finkenzeller, *RFID Handbook*, John Wiley & Sons, New York (1999).
10. D. C. Huang, F. Liao, and V. Subramanian, in *Proceedings of the Materials Research Society Spring 2002 Meeting*, MRS, (2002).
11. M. Hasan, D. Bethell, and M. Brust, *J. Am. Chem. Soc.*, **124**, 1132 (2002).
12. S. B. Fuller, *et al. J. Microelectromech. Syst.*, **11**, 54 (2002).
13. M. J. Hostetler, J. E. Wingate, C.-J. Zhong, J. E. Harris, R. W. Vchet, M. R. Clark, J. D. Longdono, S. J. Green, J. J. Stokes, G. D. Wignall, G. L. Glish, M. D. Porter, N. D. Evans, and R. W. Murray, *Langmuir*, **14**, 17 (1998).